Site amplification at the city scale in Basel (Switzerland) from geophysical site characterization and spectral modelling of recorded earthquakes.

Clotaire MICHEL[1], Donat FÄH[1], Benjamin EDWARDS[2] and Carlo CAUZZI[1]

[1] Swiss Seismological Service (SED), Swiss Federal Institute of Technology of Zurich (ETHZ), Switzerland
[2] Department of Earth, Ocean and Ecological Sciences, University of Liverpool, UK

Accepted for publication in Physics and Chemistry of the Earth, Special Issue "Advances in seismic site response: standard-practice and innovative methods", 2016, doi: 10.1016/j.pce.2016.07.005

Corresponding author
C. Michel
SED-ETHZ
Sonneggstrasse 5
8092 Zürich
Switzerland
clotaire.michel@sed.ethz.ch

Abstract:
Hazard assessment at the city scale requires a detailed characterization of the effect of surface geology on ground motion (site effects). Though this analysis is commonly achieved using geophysical site characterization and site response modelling, we propose here a complementary analysis based on amplification functions retrieved from Empirical Spectral Modelling (ESM) of earthquake recordings. We applied this method to the city of Basel (Switzerland) that benefits from a detailed microzonation and a dense Strong Motion Network with 21 modern free-field stations. We first verified the accuracy of ESM amplification functions for this region and used them to determine the bedrock interface at a site with a detailed velocity profile. While the interface between Upper and Lower Tertiary was, until now, considered responsible for the fundamental frequency of resonance in the Rhine Graben, we found that the bedrock interface in fact lies at the Mesozoic limestone. We also investigated the second peak of the H/V ratios that is clustered in a particular area of the basin where amplification is found to be different. We successfully used the ESM amplification functions to verify the microzonation of 2006 and would strongly advise the installation of strong motion stations where such studies are performed in the future. Outside the Rhine Graben, where shallow sediments are found, we propose an amplification functional form based on ESM and the fundamental frequency of resonance. Finally, we combined all our findings and generated amplification maps of the response spectrum at any period of interest for earthquake engineering. This map is proposed for a high resolution real-time implementation in ShakeMap and will be used for seismic loss assessment.

Keywords: site effects, ground motion amplification, strong motion, seismic network, ShakeMap

1. Introduction

The city of Basel is located at the south-eastern edge of the Upper Rhine Graben, at the border between France, Germany and Switzerland. Seismic hazard in the city of Basel is moderate, with uniform hazard spectra from the 2015 Swiss national seismic hazard maps of the Swiss Seismological Service (SED) indicating peak ground acceleration (PGA) at a rock horizon ($V_{s,30}$ = 1105 m/s) of 0.1 g at a return period of 475 years, and 0.5 g at 10,000 years (SED, 2015a). It was struck in 1356 by the largest earthquake known to have occurred North of the Alps, with $M_w \sim 6.6$ according to recent studies (Fäh et al., 2009). The earthquake destroyed the city and caused damage in many villages nearby. The number of fatalities was probably limited, most likely due to the numerous foreshocks that made the inhabitants leave their houses. Two fatalities have been certified, although the real number is unknown (Fäh et al., 2009). Other historical events of magnitude 5 and above occurred in 1650 and 1721, causing slight damage to the city (Schwarz-Zanetti and Fäh, 2011; Gisler and Fäh, 2011). More recently, the 2006 M_w=3.2 event induced by petrothermal activities caused widespread minor non-structural damage that led to about 9 M$ damage claims (Giardini, 2009). This is in stark contrast to a similar geothermal event that occurred in St. Gallen, Switzerland in 2013, which caused insignificant damage, as would be expected for this size of event (Edwards et al., 2015a). A key question therefore is whether amplification phenomena in Basel lead to high ground-motions.
The first qualitative microzonation study for the city was carried out by Fäh et al. (1997). It was followed in 2006 by a quantitative microzonation project (Fäh and Huggenberger, 2006) that was eventually implemented in the local building code (Fäh and Wenk, 2009). Apparent from the microzonation studies is significant amplification of earthquake ground motions, which varies according to the mechanical properties of the deposits: in the Rhine Graben, deep sedimentary layers with various degrees of consolidation have been deposited since the Tertiary, whereas outside the Graben, alluvial valleys are filled with unconsolidated Quaternary sediments. This geological complexity and the resulting site response motivated the development of site characterization techniques based on ambient vibrations (e.g. Kind et al., 2005; Havenith et al., 2007) and site response analyses based on numerical modelling (e.g. Oprsal et al., 2005).

We propose here an alternative, data-driven approach to assess the amplification of earthquake ground motions that should complement classical geophysical site characterization. Our study is motivated by the "Basel Risk Mitigation" project promoted by the Canton Basel-City between 2013 and 2015 with the goal of assessing the consequences of significant earthquakes on local school buildings, and as a pilot study for real-time loss assessment for the whole city (Michel and Fäh, 2016). Our approach is based on collecting observations of site amplification at permanent seismic stations with respect to a known reference rock profile, as detailed by Poggi et al. (2011) and Edwards et al. (2013). The main source of our data is the Swiss Strong Motion Network (SSMNet; Clinton et al., 2011; Michel et al., 2014) that was densified in the region throughout the development of this study.

In this paper, we present and discuss the amplification maps developed for the studied area. Our goal is to define the amplification of the 5% damped response spectrum in the range of the vibration frequencies of typical Swiss buildings, i.e., between 1 and 10 Hz. The amplification maps derived herein can be used as input to loss assessment studies through high-resolution earthquake scenarios and ShakeMaps (Wald et al., 1999; Worden et al., 2010; Cauzzi et al., 2015) for the Basel area.

In this paper, the Basel context is first presented including the geology, the existing microzonation studies and the SSMNet with its recent modernization and extension, completed by the installation of temporary stations within this project. We recall how the spectral modelling technique of Edwards et al. (2013) is implemented on the whole Swiss Network to retrieve information on the Fourier site amplification from recorded events. We validate this approach in Basel and propose a method to compute the site amplification for the response spectrum. Two results concerning the interpretation of the observed site amplification are presented: the interpretation of the bedrock depth and the secondary peaks in the Rhine Graben. Further, a verification of the 2006 microzonation is presented. Finally, we propose a method to combine the available data with the site characterization information to derive an amplification map for a prototype implementation in a high-resolution ShakeMap.

2. The Basel area

2.1 Geology

The area of Basel (Fig. 1) comprises two major distinct geological domains, namely the Rhine Graben and the Jura mountains. The Rhine Graben opened during the Oligocene and Miocene ages (starting 35 Myrs ago) and has been filled with thick marine and freshwater sediments since that time (Fig. 2). East of the master fault of the Graben, the Tabular Jura is made of Mesozoic rock, carved by the Rhine and smaller rivers, generally overlaid by Quaternary sediments of variable (but generally limited to 35m in most areas) thickness. In the South, the Graben extends to the folded Jura with a gradually decreasing thickness. Defining the Eastern and Southern boundaries between these two geologic features is not straightforward. They can be defined based on tectonic considerations (e.g. the location of the main Eastern fault – although this is not well defined), sedimentary considerations (e.g., presence of Tertiary sediments deposited during the extension of the Graben), or engineering seismology considerations (e.g., a jump in the resonance frequency as used in Fäh et al., 2006). In this project, we used a simplified representation of the main geological units based on the available geological maps and the 2006 microzonation map, as shown in Fig. 1.

Outside the Rhine Graben, the Quaternary sediments exceed 35 m thickness only for small areas of the Rhine valley (e.g. at station SMZW) and of the Ergolz valley (GeORG project team, 2013). According to Fäh et al. (2006), three main types of sediments can be found in this area: Pleistocene sediments are mostly made of alluvial terraces of the main rivers and are in general compact; Loess sediments, which are very soft, can be found on top of hills and were formed by wind transport; Holocene sediments are in general unconsolidated alluvial sediments (gravel and sand).

In the Rhine Graben, the Quaternary sediments are also rarely thicker than 35 m (GeORG project team, 2013). Loess hills in the South-West were distinguished from the rest of the Rhine Graben as explained in section 4.2. The Tertiary deposits (Fig. 2) are mostly marls of lacustrine origin with various degrees of consolidation filling the basin with a thickness of 50 to 1000 m in Basel (GeORG project team, 2013). They are particularly deep in the "Mulde von St-Jakob-Tüllingen" (Fig. 2), along the Eastern limit of the Graben until Reinach in the South as well as West of the Allschwil fault.
The upper Tertiary (Oligocene age) is made of various sediment types with freshwater origin superimposing seawater sediments mostly made of mudstone, both poorly consolidated (GeORG project team, 2013). The lower Tertiary is mostly constituted by a thick consolidated marl layer (formerly called Sannoisian marl).
The upper Mesozoic layers in the graben are made of massive limestone of Oxfordian age. The Lower Tertiary has been considered as the geophysical bedrock since the first studies on Basel (Fäh et al., 1997). However, we show in section 4.1 that the geophysical bedrock could be located at the top of the Mesozoic units.

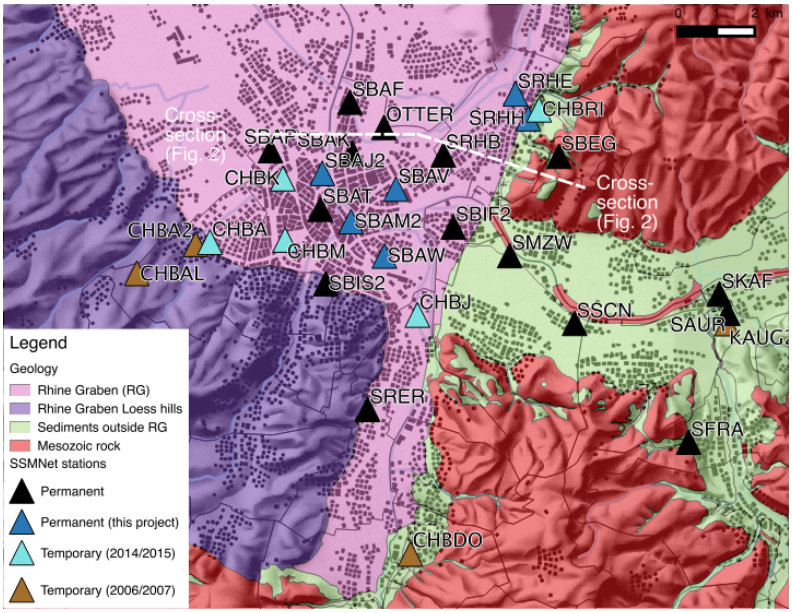

Fig. 1 Swiss Strong Motion Network (SSMNet) and simplified surface geology of the Basel area. The seismic stations are shown as coloured triangles. The cloud of light grey rectangles in the background is a simplified plan view of the Basel building stock. The elevation in the area ranges between 245 and 665 m asl. (245 to 391 m in the Graben).

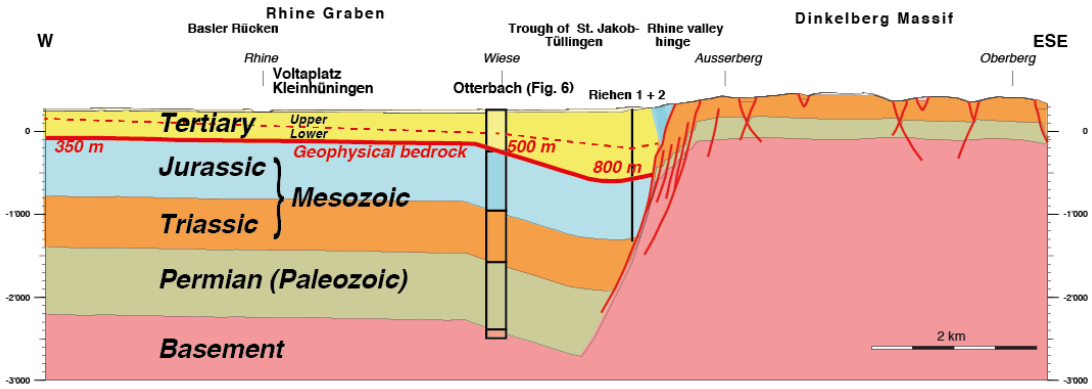

Fig. 2 E-W geological cross-section of the Basel area through site Otterbach (OTTER), see Fig. 1. The geophysical bedrock and its depth are displayed in red. Modified from Häring (2006)

2.2 Microzonation studies

Fäh et al. (1997) first proposed a qualitative microzonation of the city of Basel. They collected geological and geotechnical data, used SPT (Standard Penetration Test) to estimate the shear-wave velocity (Vs) and used the Horizontal-to-Vertical (H/V) Spectral Ratios at about 20 measurements points in the city to compute the dominant frequencies of the site response. They interpreted the fundamental frequency as the resonance of the Upper Tertiary and Quaternary layers, based on the transition between soft sediments and harder rock observed in deep boreholes. They proposed a qualitative microzonation, mostly relying on the Quaternary geology (14 criteria out of 20). This microzonation strategy was implemented in the whole city and related to amplification of earthquake ground motions in terms of EMS-98 (Grünthal, 1998) macroseismic intensity in Fäh et al. (2001). Kind (2002) further developed the use of single station measurements (255 measurement points) and introduced ambient vibration array measurements to estimate the Vs profiles at 5 sites (Kind et al., 2005). Further 2D numerical modelling was performed, and the Rhine Graben was split into five zones of assumed similar amplification. Steimen et al. (2003) studied 2D resonance in the Rhine Graben using observation and modelling and concluded that no 2D resonance was occurring in Basel but that 2D geometry was playing a role in the response of the basin. Based on the

velocity model of Kind (2002), Oprsal et al. (2005) proposed the first 3D model to simulate earthquake ground motion in Basel with an extended source using the finite difference method.

Fäh and Huggenberger (2006) proposed a quantitative microzonation for Basel that was then implemented in the local building code (Fäh and Wenk, 2009). 700 single-station measurements and 30 new array measurements were used, together with active seismic, to improve the velocity model (Havenith et al., 2007) for the city area. 1D, 2D and 3D numerical modelling was performed. For the microzonation, the city and adjacent areas was split into 14 zones (and more subzones), each of them with an amplification function in terms of pseudo spectral acceleration (PSA) and a corresponding design spectrum (Fäh and Havenith, 2006; Fäh and Wenk, 2009). The PSA amplification functions were derived as the envelope of the average modelled responses in 1D, 2D and 3D in each zone. These functions are discussed and validated in section 5.

The SED site characterization database (SED, 2015b; Fig. 3) therefore contains a large amount of data collected in the Basel area from passive single station and/or array measurements as well as from active geophysical measurements from the different projects carried out in Basel, as first presented by Havenith et al. (2007). Since then, new data have been gathered after the 2006 geothermal events (Ripperger et al., 2009) and within the framework of the current project.

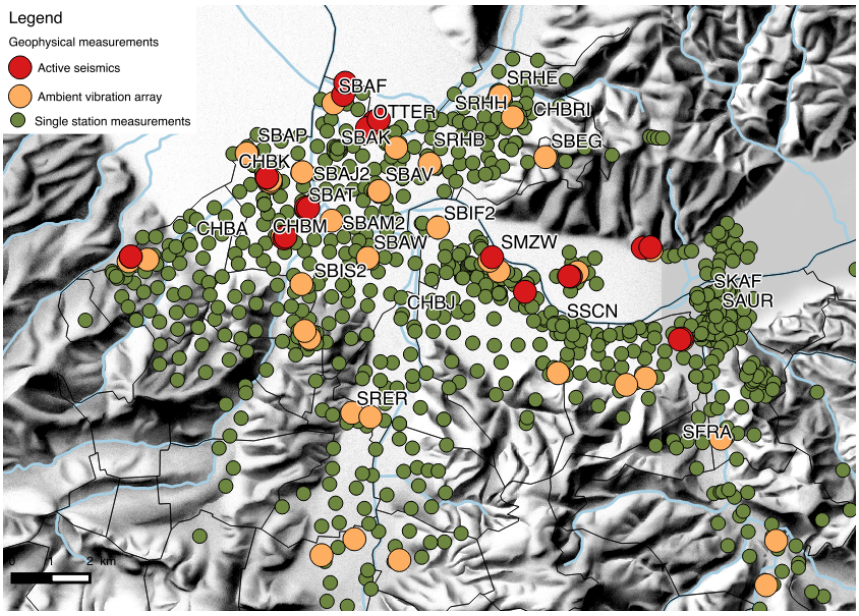

Fig. 3 Digital elevation model of the area of Basel and distribution of the measurements available in the SED site characterization database (SED, 2015b).

2.3 SSMNet and temporary seismic networks in Basel

With an average interstation distance smaller than 2 km, the Swiss Strong Motion Network (SSMNet) in the Basel area is remarkably dense (Fig. 1). It currently comprises 21 permanent free-field stations, continuously recording and transmitting data to the Swiss Seismological Service (SED). The development of the SSMnet in Basel started in the early 1990s, with 9 low-gain accelerometer stations with dial-up communication installed between 1990 and 1998. In the framework of the aforementioned 2006 microzonation project, 8 modern broadband accelerometer stations with continuous telemetry were installed in 2005/2006. Another 2 modern stations were installed in 2007/2008. Since 2010, 5 supplementary stations have been modernized or newly installed in the framework of the national renewal project (Michel et al., 2014) (SBEG, SRER, SBAK, SBIF2, SSCN). Between 2013 and 2015, 6 additional high-quality (Cauzzi and Clinton, 2013) free-field strong-motion stations (SBAM2, SBAJ2, SBAV, SBAW, SRHE, SRHH) were installed through the Basel risk mitigation project. Five of these new stations are located close to school buildings. 1D velocity profiles were determined for all the newly installed permanent stations based on array measurements of ambient vibrations as proposed by Michel et al. (2014).

The information related to the SSMNet stations in Basel, and especially their site characterization, is stored in the SED (Swiss Seismological Service, 2015) station database, and is available through a web interface at *stations.seismo.ethz.ch*.

In addition to the permanent network, five temporary stations (CHBA, CHBJ, CHBK, CHBM, CHBRI) were installed and were operational from August 2014 to September 2015 (Fig. 1). They were fully integrated in any routine operations of the national monitoring network including real-time and rapid delivery of earthquake locations, magnitudes and associated products. During one year of operation, the temporary stations recorded 2 to 13 events with a sufficient signal to noise ratio across the distance and frequency range defined by Edwards et al. (2013). Station CHBK was located in the noisiest area of the city and therefore recorded only 2 events, while stations located in quiet suburbs recorded about 10 events. The seismicity was low during the recording period. The network clearly recorded all events with $M_L > 3$ within Switzerland and surrounding regions (see Diehl et al., 2015). In 2006/2007 a temporary network was also installed to monitor the seismicity induced by the Deep Heat Mining Project (Ripperger et al., 2009).

3. Site Amplification from Earthquake Spectral Modelling (ESM)

3.1 Empirical Spectral Modelling and validation

Following Edwards et al. (2013), the Fourier amplitude spectra of recorded earthquakes at each station of the network are modelled in near real-time (i.e., within minutes of real-time earthquake detection and location). All signals with sufficient signal-to-noise ratio (SNR>3) are used to retrieve information about the source (moment magnitude M_W and stress parameter), the path (geometrical spreading and anelastic attenuation) and the average amplification A_j at each site j. The residuals at each frequency of the modelling with respect to the observations are assumed to be the frequency-dependent site amplification function $a_j(f)$ at each site. The elastic ESM amplification function is retrieved by statistical analysis over a large number of recorded events of $A_j \times a_j(f)$. The anelastic ESM amplification function, relative to the reference rock model $A_j \times a_j(f) \times e^{-\pi f \Delta\kappa_j}$ is also computed, with $\Delta\kappa_j$ defining the difference in attenuation between site j and the theoretical reference rock site. However, the large uncertainty in $\Delta\kappa_j$ imposes a large standard deviation to the anelastic ESM function at high frequencies (*e.g.* Fig. 4; Edwards et al., 2015b). The reference of these amplification functions is the Swiss reference rock model of Poggi et al. (2011).
Although Edwards et al. (2013) showed that the ESM functions are usually reliable, the ESM results may be biased until stations have several recordings. The shape of the amplification function $a_j(f)$ is already reasonably constrained by few events, but the average amplification A_j may be uncertain if the recorded events are not adequately spatially distributed. Many events recorded in Basel were induced by the geothermal Deep Heat Mining Project and recorded at less than 5 km from the rupture (Deichmann and Giardini, 2009). Events pertaining to induced sequences occur at about the same location with similar source mechanisms and radiation of energy for a given station. This breaks the assumption of the computation of the ESM amplification, which does not include radiation pattern, instead assuming a homogeneous distribution of events to ensure no bias due to source effects. The ESM function retrieved at some temporary stations installed during the geothermal sequence were considered unreliable for this reason and therefore not used in this study.

Moreover, in our computations the average amplification (A_j) values of Basel stations SBAP, OTTER, SBAT, SRHB and SMZW are assumed to be known *a priori* along with those of 22 other regional stations that were used to define the Swiss reference rock model of Poggi et al. (2011). Note that A_j values for the other stations are inverted for each event. We studied the *a posteriori* average amplification A_j computed for each event and aforementioned station as the average observed spectrum divided by the modelled spectrum without site term. Our goal is to track possible biases in these amplification function due to the geothermal events (Deichmann and Giardini, 2009). As a result, we found that the only station with non-normally distributed $\ln(A_j)$ is OTTER, located at the epicentre of the geothermal events, showing that the radiation patterns of the induced events have an impact on the average amplification value fixed for this station. Therefore, only the natural events are used in the following. The correction factors computed for the amplification function at the fixed stations are therefore defined as the mean correction of all natural events without outliers (correction factors greater than 2.5). The obtained correction factors are summarized in Tab. 1. The only large correction (36%) is for station OTTER. Station SBAP shows a correction of 12%, which is not a large value when considering the uncertainties of the amplification function. The others are 7% or less indicating that the A_j values retrieved in Poggi et al. (2011) were accurate.

Tab. 1 $\boldsymbol{A_j}$ correction factors with respect to $\boldsymbol{A_{j,fixed}}$ (Poggi et al., 2011) ($\boldsymbol{A_j/A_{j,fixed}}$) of ESM for the stations in Basel with available $\boldsymbol{A_{j,fixed}}$

Station	A_j correction factor ($A_j/A_{j,fixed}$)
SBAP	0.88
OTTER	1.36
SBAT	1.04
SRHB	1.07
SMZW	1.02

Moreover, during the estimation procedure, a trade-off between site amplification terms A_j and $\Delta\kappa_j$ may also result in deviations in parts of the amplification function. In the following, we verify that this issue is not affecting the amplification functions by comparing the ratios of the ESM functions with the Fourier standard spectral ratios (SSRs; Borcherdt, 1970) of the recordings of natural events with respect to station SRHB, located in the Rhine Graben (Fig. 4), and station SKAF, located outside (Fig. 5). While not a rock station, SRHB, located in the centre of the basin, was chosen for its relatively flat amplification function. SKAF is a rock station, however it is located relatively far from the rest of the network (Fig. 1). The numbers of recordings given in Figs. 4 and 5 correspond to those of the SSR curves and are modulated at low and high frequencies by the signal-to-noise ratio. Note also that fewer event recordings are available for the pairs of stations used to compute the SSRs than for the ESM at single stations, so that reliable SSRs could not be computed for all station pairs. Even so, the match is good for most of the stations. The A_j correction proposed above improves the results, especially for OTTER station (Fig. 4a). The trade-off with $\Delta\kappa_j$ may be the reason for the slight mismatch at station SBIS2 (Fig. 4c).

As a conclusion, the ESM functions, even though sometimes based on few earthquakes only, are reliably depicting the amplification at each SSMNet station. Biases due to the distribution of events can however still be present in both ESM and SSR and will be removed once more recordings will become available. Amplification analysis through ESM overcomes the drawbacks of the Standard Spectral Ratio technique as use for instance by Ullah et al. (2013) for the same purpose. SSR requires a reference station on rock and assumes that the effects of propagation between the stations is negligible. As previously mentioned, ESM also allows the use of more recordings.

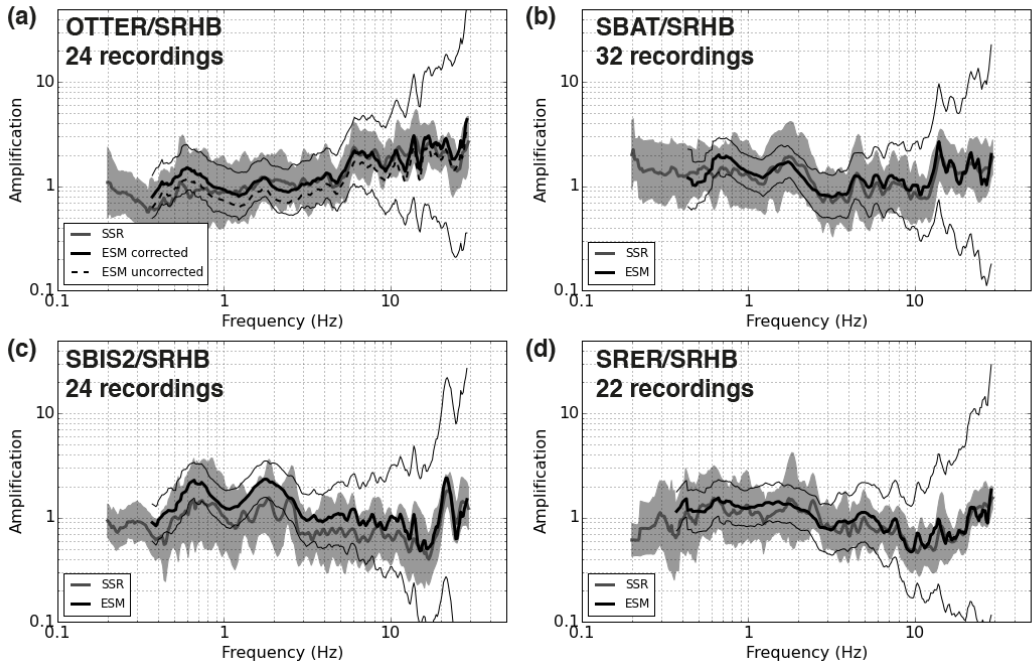

Fig. 4 Comparison of standard spectral ratios (SSRs, grey lines and grey shading) and ratios of anelastic ESM functions (black lines), with their respective standard deviations, for stations in the

Rhine Graben with respect to SRHB. For OTTER station, the ESM ratios without correction (dashed line) are displayed as well.

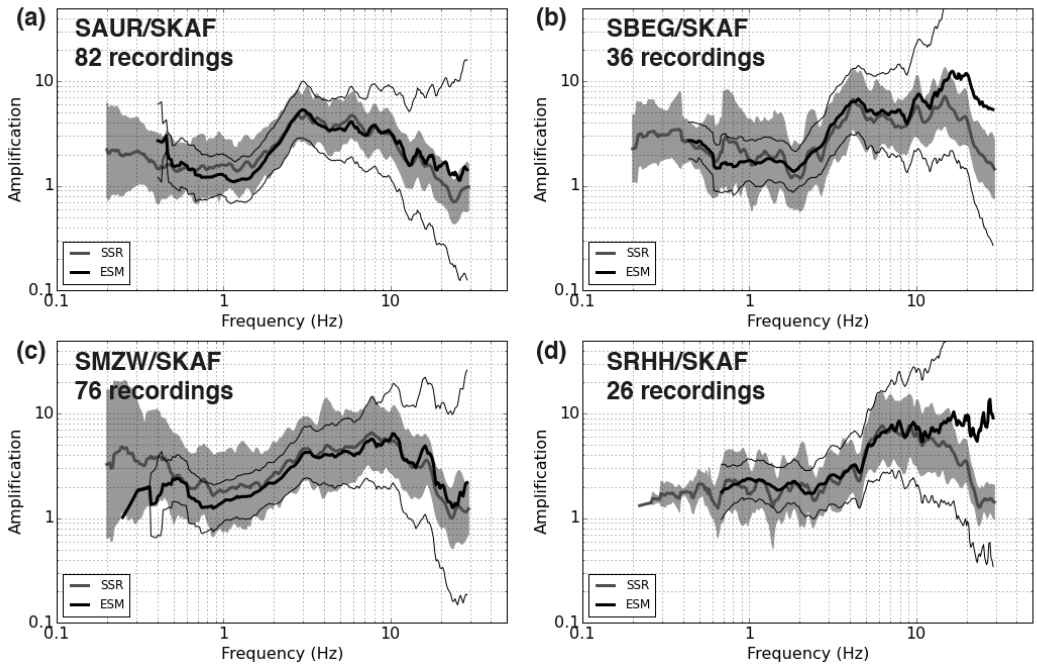

Fig. 5 Comparison of standard spectral ratios (SSRs, grey lines and grey shading) and ratios of anelastic ESM functions (black lines), with their respective standard deviations, for stations outside the Rhine Graben with respect to SKAF.

3.2 ESM amplification in the response spectral domain

Whilst widely used in seismology, Fourier spectra are not as commonly used in earthquake engineering, where the seismic demand is traditionally specified in terms of damped response spectra, especially pseudo spectral acceleration (PSA). We therefore also computed the ESM amplification functions in terms of PSA using Random Vibration Theory (RVT) (Cartwright and Longuet-Higgins, 1956; Liu and Pezeshk, 1999). RVT provides a theoretical framework for passing from the Fourier domain to the response spectral domain; effectively a short-cut to producing complete time-domain stochastic-phase accelerograms (Boore, 2003) when only peak values of oscillation are required (e.g., Bora et al., 2015). This approach is often used in engineering seismology for the adjustment of ground motion prediction equations (e.g., Campbell, 2003; Edwards et al., 2016). Simulations for a given scenario of magnitude 5 at 50 km were generated using the Swiss Stochastic Model (Edwards and Fäh, 2013) with (a) anelastic (i.e., including κ_0) Fourier amplification at the reference rock model of Poggi et al. (2011), and (b) site-specific anelastic Fourier amplification (Figs. 4 and 5). The resulting response spectra from (a) and (b) were then used to compute the amplification function between the site and the Swiss Reference in the response spectral domain. We found out that this PSA amplification was insensitive to the scenario (magnitude, distance) used for the range of interest to engineering design (M≥5; R<100km). Future improvements should however include an assessment of the uncertainties on these functions. At long periods (T > 0.2 s) the response and Fourier amplification are similar, however, at short periods (T < 0.1 s) the Fourier and response spectral amplification differ significantly (Bora et al., 2016). While the Fourier ESM amplification functions are used to better understand the nature of site effects in sections 4, PSA ESM amplification functions are used in sections 5 and 6 to quantify the amplification for engineering applications.

4. Re-interpretation of site characterization data

In this study, two new key findings concerning the site characterization in Basel are presented and discussed: the interpretation of the bedrock depth and the distribution of the second peak in the H/V data.

4.1 Bedrock depth

At Otterbach (station OTTER), a sonic logging of Vp data from 30 m to 2500 m depth was made available by the DHM project (Häring, 2006). Data from a second borehole of the same project (BS-1) between 450 m and 5000 m depth and located at about 1 km to the NNW allow the extension of the data (Vp and Vs) to greater depths. The two logs are shifted in depth by 102 m due to the shape of the basin. The Otterbach sonic logging provides the P-wave velocity in the borehole at 5 cm intervals. We interpreted these data using homogeneous layers based on the observed velocity variations and geology logs (Häring, 2006). Density was also obtained from the borehole logging. We estimated the S-wave velocity (Fig. 6) based on a constant Vp/Vs ratio of 1.9 (Poisson ratio of 0.31) in the sedimentary layers and 1.75 (Poisson ratio of 0.25) in the crystalline basement. These values were obtained from data of the second borehole but could be larger at the surface. Other geophysical measurements confirmed this model except for the first 70 m, where the shear-wave velocity decreases rapidly, and therefore the Poisson ratio increases. At this site OTTER, the Quaternary sediments are 18 m thick (velocity not measured). The Upper Tertiary layers extend to 273 m depth and have a shear wave velocity of about 1000 m/s. The Lower Tertiary unit has a velocity of about 1600 m/s and the Mesozoic, at 500 m depth, a velocity of about 2400 m/s. The shear wave velocity in the crystalline basement, starting at 2650 m depth, is 3400 m/s.

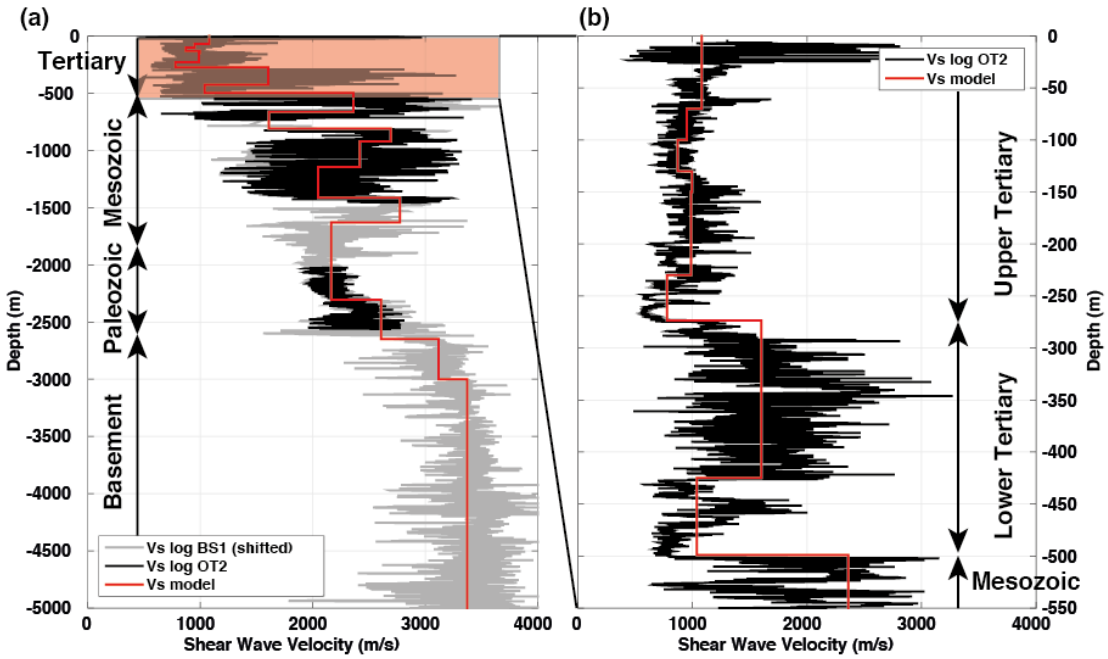

Fig. 6 Vs profile at site Otterbach (OT2) from borehole logging over the whole available depth (a) and zoom over the 550 first meters (b). Velocity data from borehole BS 1 are vertically shifted 102 m to reflect the observed differences in the layer depths.

Following Edwards et al. (2013), we used the simplified Vs model of Figure 6 to compute the elastic SH transfer function. We corrected it to the Swiss reference rock of Poggi et al. (2011) by computing the impedance contrast between the velocity of the lowermost layer and the Swiss reference (Eq. 7 of Edwards et al, 2013). We compared the corrected SH transfer function to the ESM amplification function derived at OTTER (Fig. 7) and observed a good agreement between the empirical and the numerical approach as to both the frequency and amplitude of the fundamental peak. Discrepancies at higher frequencies are due to the lack of data within the first 70 m of the soil column. By removing the rock layers one after the other at the bottom of the simplified Vs profile, we identified that the interface between the Lower Tertiary unit and the Mesozoic layers at 500 m depth controls the fundamental frequency of the site response, between 0.4 Hz and 1 Hz. The geophysical bedrock is therefore the Mesozoic limestone at this site. As a result, future numerical models of the site should account for this interface.

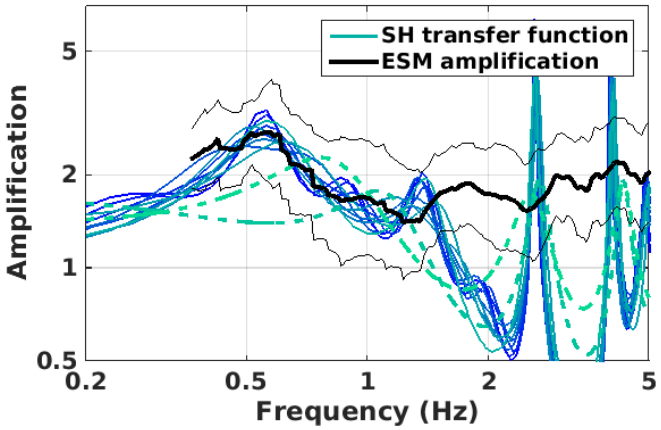

Fig. 7 Comparison between the observed ESM function at OTTER station (black curves) and the SH transfer function from the 1D velocity model from the sonic logging (blue curves), gradually reducing the number of layers at the bottom of the profile. The results are similar until the Mesozoic layer is removed (dashed lines).

4.2 Second peak in the H/V ratios

Nearly all the single-stations recordings available in Basel were homogeneously reprocessed using the H/V method (2200 points). The recording quality of this dataset is heterogeneous since the measurements were performed between 1997 and 2014. All points in the city-centre were re-picked including second peaks, when existing. While the fundamental peak is related to the interface with the bedrock, secondary peaks may relate to intermediate layering and may also play an important role in the amplification. For instance, at the permanent station SBIS2 (Fig. 4c) a peak at 2 Hz in the amplification function can be related to a peak at the same frequency in the H/V curve. It is observed that this peak is stable with time in the H/V ratios of SBIS2. Fig. 8a shows the map of these second peaks. Some high-frequency values (above 10 Hz, white to blue) can be recognized at various places in the basin, with a high variability. These sites are characterised by shallow low-velocity layers, in some cases anthropogenic infill. Second peaks at lower frequencies (below 10 Hz, white to red) are found only in the Loess hills in the South of Basel (yellow area), which justified segregating the Rhine Graben into 2 zones. The lowermost frequency of the second peaks is about 2 Hz but it is difficult to map it precisely because the peak has a small amplitude and is not apparent everywhere. Its frequency value is not correlated with the thickness of the Quaternary layer (Fig. 8b). Moreover, the array analyses available in Basel do not show any noticeable velocity contrast between Tertiary and Quaternary layers. The second peak is partly reproduced in the microzonation of 2006 by the 2D model (Fäh and Havenith, 2006) but not by the 1D SH transfer function. At site CHBAL, it is also not reproduced by 1D site characterization (site Allschwil 1 in Havenith et al., 2007). A topographic origin for this second peak cannot be excluded but is unlikely (Burjanek et al., 2014). However, additional work, including simulation with a reliable 3D model capable of taking into account the local generation of surface waves and focusing and defocusing effects, is necessary to provide a final interpretation

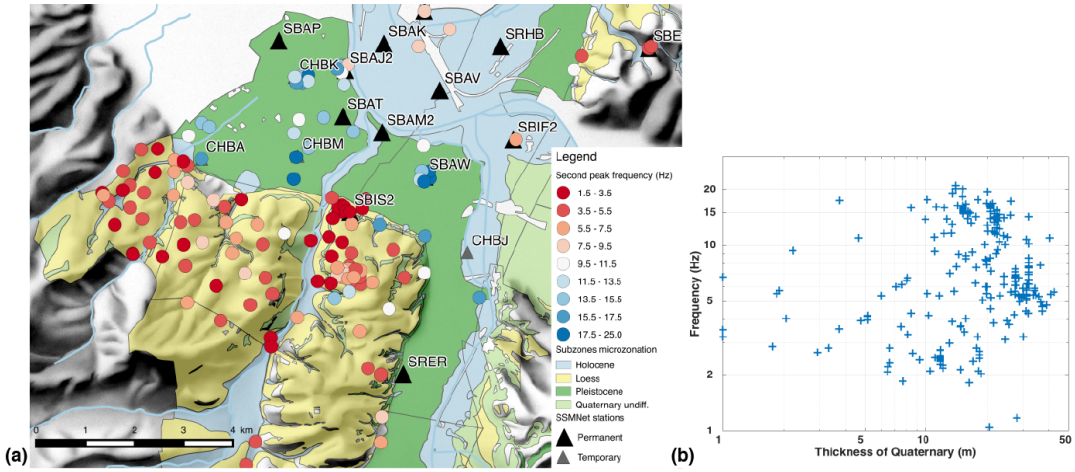

Fig. 8 Second peak in the H/V ratios in the Rhine Graben in Basel. a) Map of the frequency distribution related to surface sediments as mapped by the 2006 microzonation; b) Frequency values with respect to the thickness of the Quaternary sediments (GeORG project team, 2013).

5 Validation of the microzonation of 2006

In order to validate the PSA amplification functions derived from the microzonation, we first changed the reference of each of them to the generic Swiss rock (Poggi et al., 2011) by computing the correction from the impedance contrast between the reference of Fäh and Havenith (2006) and the Swiss reference velocity profiles expressed as the ratio of their quarter-wavelength velocities. We did not account for differences in the anelastic attenuation. These curves are compared to the PSA ESM amplification functions of stations located in each zone, if any.

The zone "Basel Nord" includes the city centre and hosts a large number of SSMNet stations (Fig. 9a). Its amplification function shows a peak around 1 Hz. Although the amplitudes match with the observations, a large variability among the observed ESM functions is observed. Some stations in the North-East (SBAF, OTTER) show lower amplifications. The sub-zones Holocene and Pleistocene show a difference above 2 Hz that does not correspond to any feature in the ESM function. The eastern part of the Rhine Graben (zone "Rheingraben Ost") shows an amplification function in the microzonation with amplitudes decreasing from 3 at 0.5 Hz to 2 at 10 Hz (Fig. 9b). Most of the stations in the zone show similar amplification, with little variability.
The Loess hills are represented by the zone "Basel West" located western from the Allschwil fault and the zone "Rheingraben West" that have a comparable amplification function with an average amplitude of 3 (Fig 9c). Stations CHBAL and CHBA2 show similar amplitudes though the second peak in the H/V ratios around 4 Hz induces a peak that is not covered by the amplification function proposed for the microzonation. The ESM function of station SBIS2 matches well with the amplification of the microzonation, including the second peak at 2 Hz.

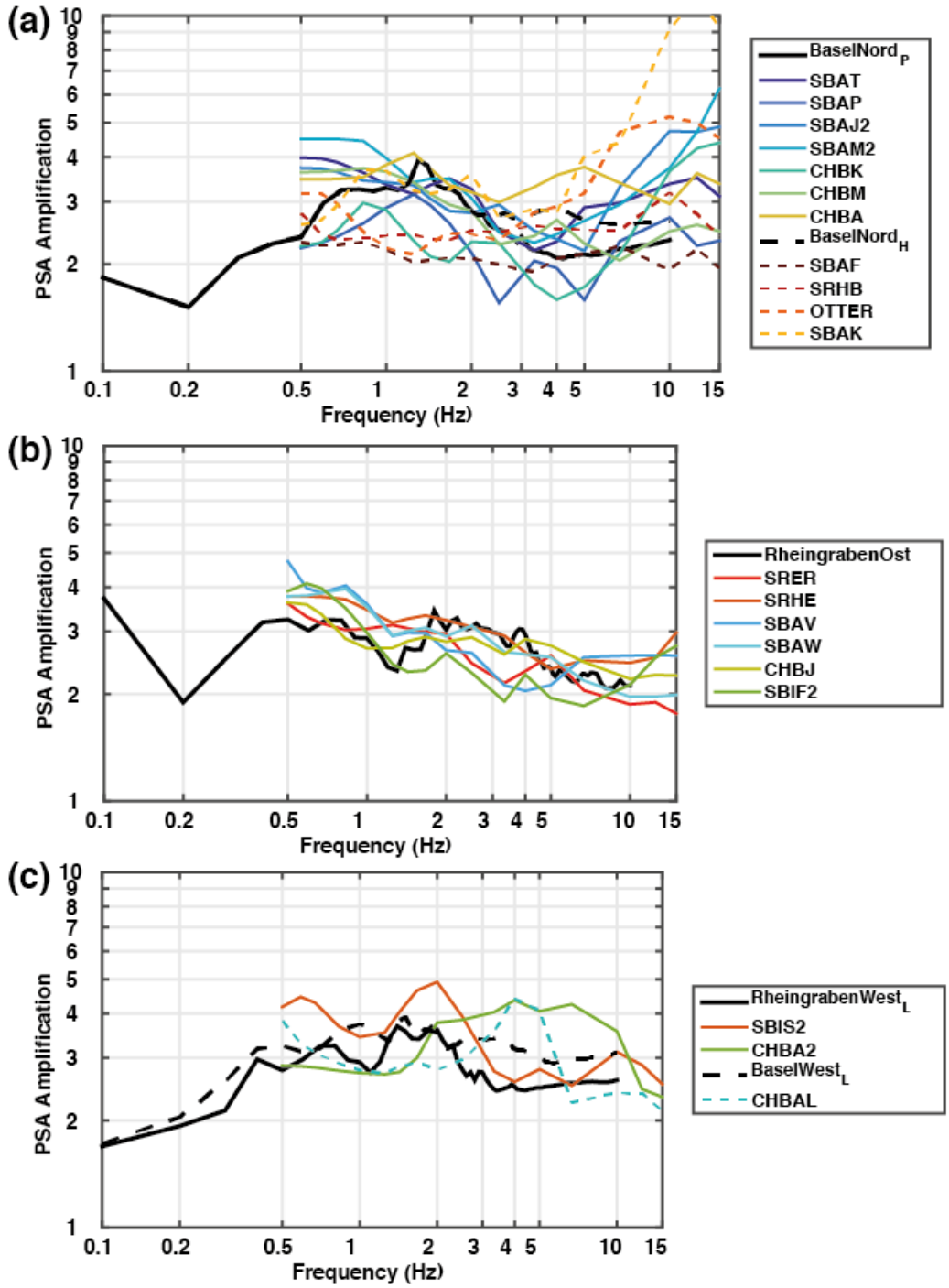

Fig. 9 Comparison of the PSA amplification in different zones of the 2006 microzonation inside the Rhine Graben (black curves) and PSA ESM functions of stations located in the corresponding zones (coloured curves). a) Zone "Basel Nord"; b) Zone Rheingraben Ost"; c) Zones "Rheingraben West" and "Basel West" (Loess hills). Subscripts P (Pleistocene), H (Holocene) and L (Loess) denote the subzones.

Outside the Rhine Graben, the zones of microzonation aggregate areas with properties strongly varying over short distances. They show a ramp function increasing from unity to about 3 (Fig. 10). The resonance frequency at the stations' sites strongly influences the amplification function so that the comparison between microzonation and stations is difficult. However, amplification up to 2 Hz matches in general while at higher frequencies, the peak amplification of the ESM functions may exceed notably the values from the microzonation. The rocky subzone "Basel Ost HF" (Fig. 10) overestimates the amplification between 1 and 10 Hz observed at station SKAF. This station shows deamplification with respect to the reference rock and

has therefore higher Vs values than the reference model (Vs_{30}=1100 m/s). It corresponds to recently eroded rock by the Rhine river.

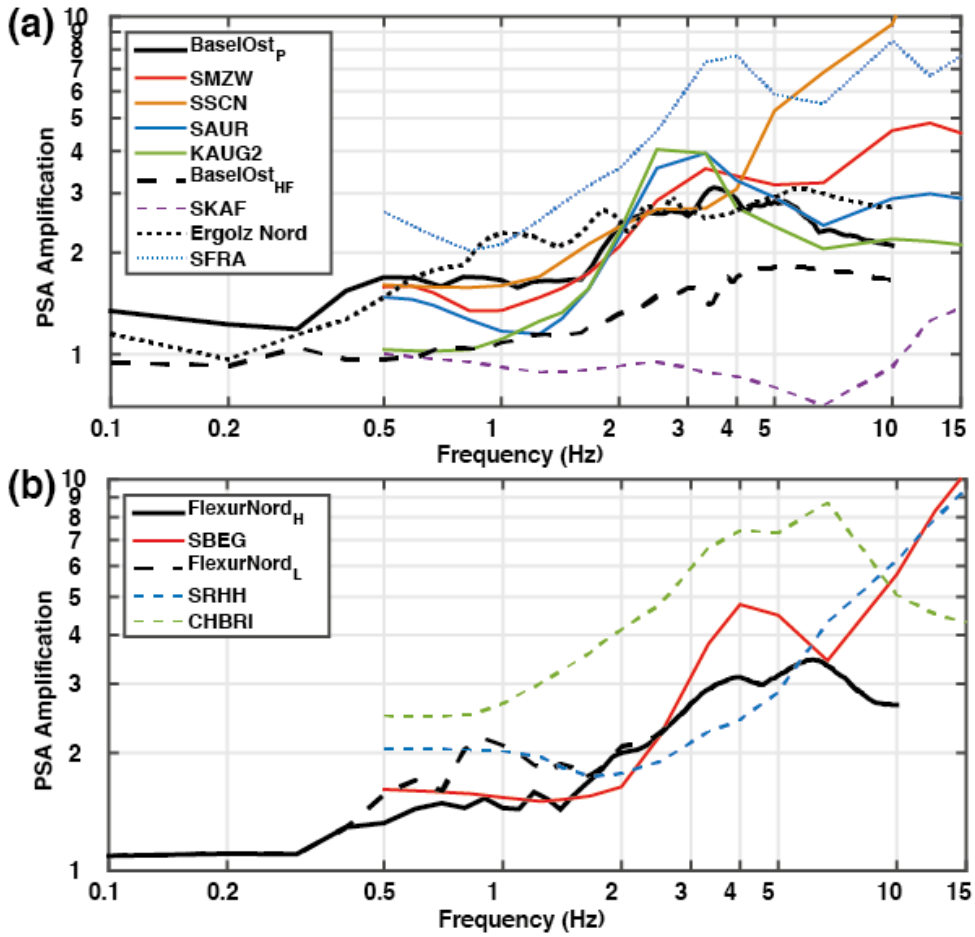

Fig. 10 Comparison of the PSA amplification in different zones of the 2006 microzonation outside the Rhine Graben (black curves) and PSA ESM functions of stations located in the corresponding zones (coloured curves). a) Zone "Basel Ost"; b) Zone "Flexur Nord". Subscripts P (Pleistocene), H (Holocene) and L (Loess) identify the subzones.

As a conclusion, the microzonation and the observed ESM amplifications match well overall, particularly in the Rhine Graben (Fig. 9) where they are relatively homogeneous. Some high-frequency amplifications, for instance in the Loess hills in the South of Basel, are however not reproduced. Outside the Rhine Graben (Fig. 10), a larger variability is expected and observed, so that the microzonation hardly models the amplification. In the area outside of the Rhine Graben, for a high resolution amplification mapping, a single amplification function per zone is not enough due to the variability of the fundamental frequency of resonance.

6 High-resolution amplification maps and application

As shown in section 5, the amplification maps derived within the framework of previous microzonation studies can be considered as suitable, though they could be improved using newly available data. Therefore, we propose here a new method to derive amplification maps based on observed ESM functions in PSA. According to the results in section 5, the inner and outer portions of the Rhine Graben are treated separately in the following.

6.1 Amplification in the Rhine Graben

The amplification in the Rhine Graben is mostly controlled by the deep sediments and varies smoothly as shown by the ESM functions (Fig. 9). Michel et al. (2014) showed that this could indicate 2D or 3D site effects. However, no 2D resonance is expected, but only generation of surface waves at the edge of the basin (Steimen et al., 2003; Michel et al., 2014). The depth of the sediments, increasing towards the east (trough of St-Jakob Tüllingen), controls the fundamental frequency, between 0.4 and 1 Hz, that is not prominent in the ESM amplification functions. It should be noticed that the ESM function is not available below 0.6 Hz due to a lack of recordings of large earthquakes.
As shown previously, a noticeable exception is observed at site Bruderholz (SBIS2) that shows large amplifications with a second peak at 2 Hz and to a lesser extent at sites CHBAL and CHBA2, also located on the Loess hills in the South of Basel. This peak is discussed in section 4.2 although no final interpretation could be found. We have therefore to rely on the empirical observation, based on homogeneous H/V curves and ESM amplification, that the amplification is larger in the Loess hills. The site response in this area remains poorly understood compared to the rest of the Graben.

6.2 Amplification outside the Rhine Graben

Outside the Rhine Graben, the depth of the Quaternary sediments is generally limited though the resonance frequency can be as low as 1 Hz in some areas. The assumption of a single layer over the bedrock can be made there as 1D site characterization is generally capturing the amplification at the sites (Michel et al., 2014). Site-response is then controlled by the thickness of the sediments and their S-wave velocity. The fundamental frequency of resonance f_0 has the property to integrate these two parameters. Although it cannot explain the whole amplification, it is expected to capture its main features. Therefore, we studied the amplification functions normalized by the fundamental frequency of the site f_0, obtained through H/V ratios.

Cadet et al. (2012) proposed a generic model called SAPE for amplification functions based on f_0, Vs_z (travel time average S-wave velocity over the z first meters) or any combination of these parameters, based on Japanese sites. We compared their model using f_0 only to our observations from ESM, normalized by f_0 (Fig. 11). Moreover, we compared them to the amplification curves from the microzonation for zones outside the Rhine Graben. The first peak in the amplification function was considered as the fundamental frequency f_0. The shapes of the obtained functions are comparable.

The peak amplitude of the ESM functions is variable but it is not clearly correlated with parameters such as the peak amplitude in the H/V ratios, f_0 or the sediment type. It indicates variations in the quality of the surface sediments that cannot be represented with available proxies. The microzonation and the SAPE function show lower amplitudes than the ESM curves and a smoother function. The SAPE model is based on the average over a large amount of different sites that do not fully reflect the situation in Basel. Moreover, the SAPE model depends on f_0 with decreasing amplitude at the peak with increasing f_0, while we observed the opposite.
The amplitudes after the peak are generally lower for the microzonation than for the ESM functions. In the ESM function, the amplification after the peak is controlled by the site-specific anelastic attenuation $\Delta\kappa_j = \kappa_{0j} - \kappa_{0,Ref}$. The observed $\Delta\kappa_j$ values using ESM are negative indicating a lower attenuation compared to the Swiss Reference rock, which corresponds to amplification as expected in shallow sediments over a stiff bedrock. Conversely, $\Delta\kappa_j$ values in the Rhine Graben are generally positive and correspond to stronger attenuation with respect to the reference. However, the uncertainty has the same order of magnitude as the mean (Edwards et al., 2015b) so that the observed variability in the ESM function after the peak cannot be completely trusted.

An amplification functional form is therefore proposed as the average of the available ESM amplification functions outside the Rhine Graben (Fig. 11). It is extended at low frequency using the curve from the microzonation. This function can be used in combination with the fundamental frequency of the site to predict the amplification at any frequency (see next section).

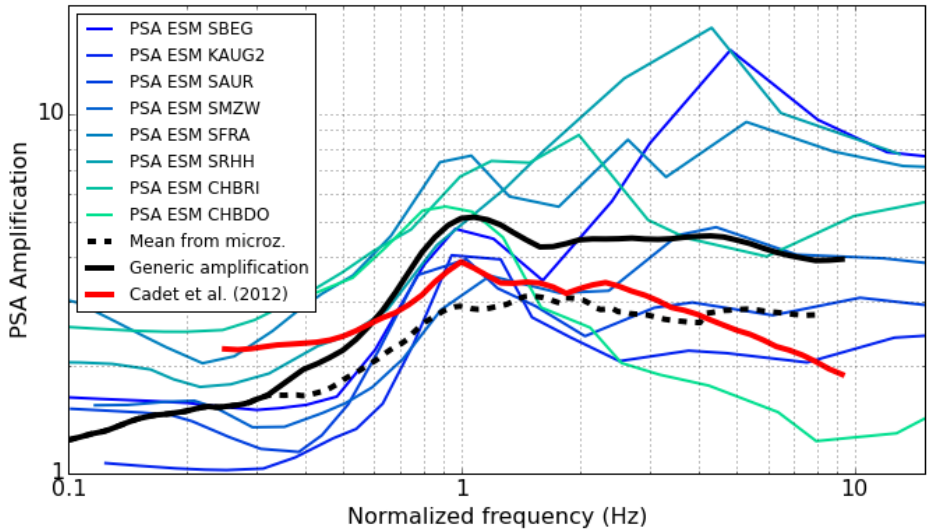

Fig. 11 Amplification function normalized by the fundamental resonance frequency of the site f_0 (purple to green curves: ESM functions; solid black line: selected functional form; dashed black line: mean of the microzonation amplification functions; red line: SAPE function of Cadet et al., 2012).

6.3 Computation of amplification maps

We showed in the previous sections that the average amplification does not vary significantly in the Rhine Graben where many stations are available. Therefore, we performed a spatial interpolation of the station ESM amplification in the Rhine Graben. For that purpose, we used the robust nearest neighbour method that separates the space into Voronoi cells around the known points and assigns one value per cell (Cressie, 1993).
We also showed that the Loess hills in the South and the West of Basel were exhibiting different behaviour (secondary peaks, higher amplification) so that data in this area is interpolated separately from the rest of the basin. Only 3 stations with very different amplification functions are available in this area so our interpolation using the nearest neighbour method remains uncertain.

Outside the Graben, we used the amplification functional form developed in the previous section (solid black line in Fig. 11) to compute the amplification at each available f_0 values. The results are interpolated over the whole area except in zones considered as rock (in red in Fig. 1) using the inverse distance weighting (IDW) algorithm (Cressie, 1993). IDW allows a simple and smooth interpolation based on the values at a given number on neighbours weighted by their distance. However, depending on the weighting function and the distribution of available data, it may create unrealistic artefacts. The power p used to weight with respect to distance can be modulated. A large value (16) simulates the nearest neighbour method. A value of 2 is used here as a trade-off.

The final amplification maps, which quantify the site effects, are displayed in Fig. 12 and compared to the amplification of the 2006 microzonation at period of 0.3 and 1 s (frequencies of 3.3 and 1 Hz, respectively). Rock areas are set to the default unit value for each method. One can notice that the change in the rock reference for the microzonation affects this value at 0.3 s, leading to an insignificant de-amplification. A grid size of 40 m has been selected for the computation as a good trade-off regarding the density of available data. It should be noticed that the microzonation is available in a limited area, for instance not outside the Swiss border, where a default value of 1 is displayed. The amplification maps resulting from this study show similar orders of magnitude compared to the 2006 microzonation. However, the Rhine valley outside the Rhine Graben shows larger values than the microzonation at 0.3 s but lower at 1 s. The interpolated map extends also to the right riverside of the Rhine (Germany) where data is also available. Towards west (France), however, the results are extrapolated.

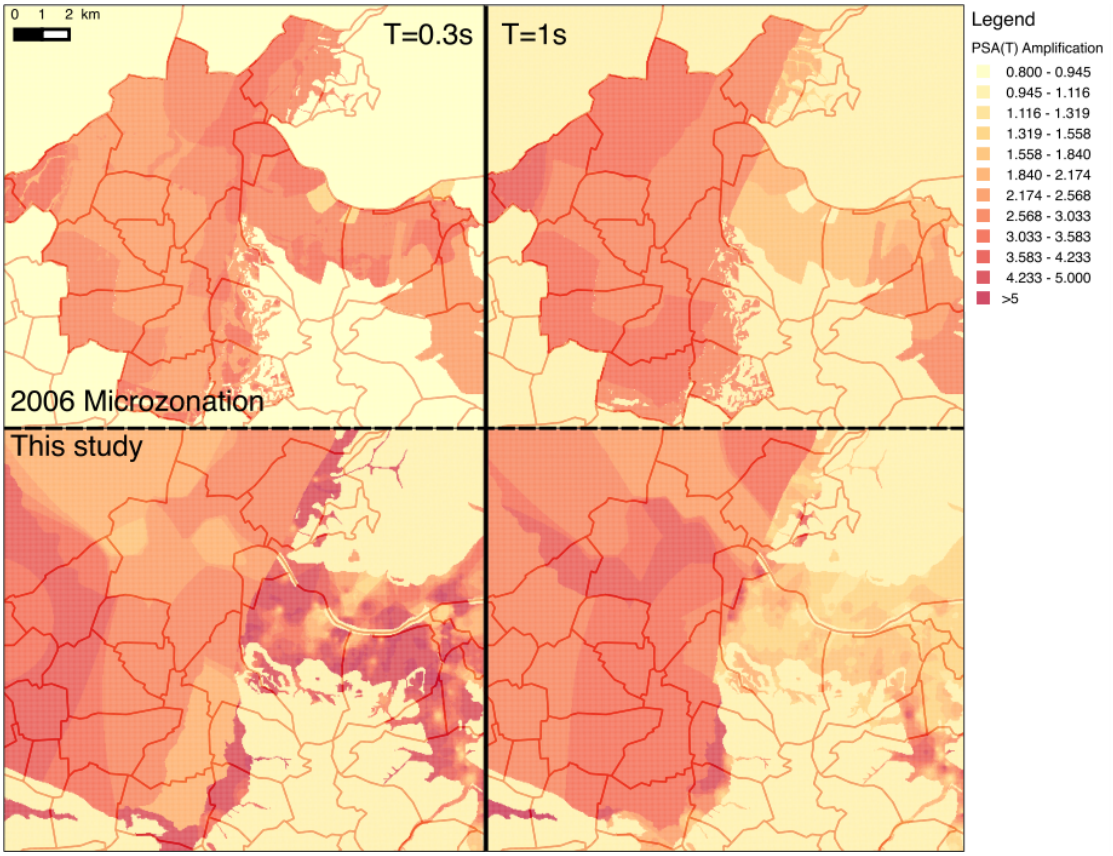

Fig. 12 Amplification maps in Basel in terms of spectral acceleration at 0.3 s and 1 s based on the 2006 microzonation and the new interpolation.

6.4. Towards a high-resolution implementation in ShakeMap

ShakeMap is a worldwide-known scientific and technical framework that delivers near real-time earthquake shaking maps based on recorded and predicted ground-motions, spectral amplitudes and macroseismic intensity levels, including amplification due to local site effects. ShakeMap was first developed for significant earthquakes in California (Wald et al. 1999) and is nowadays routinely used in many other regions in the United States and worldwide (Worden et al., 2010) in order to optimize emergency response capabilities and information dissemination following relevant earthquakes. The latest nation-wide implementation for Switzerland is documented by Cauzzi et al. (2015). Consistent with engineering seismology studies in Switzerland, it uses the Swiss stochastic model of Edwards and Fäh (2013) and a strategy to site amplification based on expected macroseismic intensity increments with respect to median intensity predictions for the country (Fäh et al., 2011). The high-resolution (40 m) amplification maps derived in the previous section can be used in the future for a local ShakeMap implementation as selectively described in the following.

In Swiss ShakeMaps (Cauzzi et al., 2015), macroseismic intensity I is converted from peak ground velocity (PGV) based on Faenza and Michelini (2010). For conversion of PSA levels, one can rely on Faenza and Michelini (2011) for vibration periods equal to 0.3, 1 and 2 s. The low-energy events characterising the seismicity of Switzerland and the typical vibration frequencies of the Swiss building stock led us to choose 0.3 s as a good candidate for this exercise. The conversion equation of Faenza and Michelini (2011) is given by:

$$I = 1.24 + 2.47 log_{10}[PSA(0.3s)] \quad (1)$$

The relationship between the intensity increments ΔI and the amplification of the spectral acceleration at 0.3 s ($A^{0.3s}$) is then:

$$\Delta I = 2.47 log_{10}\left[\frac{PSA(0.3s)}{PSA_{ref}(0.3s)}\right] = 2.47 log_{10}[A^{0.3s}] \quad (2)$$

where PSA_{ref} denotes the PSA at the Swiss reference rock model.

Fig. 13 shows the amplification yielded by Eq. (2) and the previously described spatial interpolation schemes compared to the amplification data used for the national ShakeMaps, based on macroseismic data and surface geology (Cauzzi et al., 2015). As apparent from the figure, the use of new, high-resolution data results into a significantly reduced amplification on rock-like ground and more homogeneous amplification levels in the Rhine Graben. A shaking scenario of the possible repetition of the 1356 M_w 6.6 event is shown in Figure 14. This purely predictive ShakeMap uses the amplification data of Figure 13(a) and the source geometry of Ferry et al. (2005) and Cauzzi et al. (2015). Predicted intensity reaches degree IX as reported in the ECOS-09 catalogue (Fäh et al., 2011).

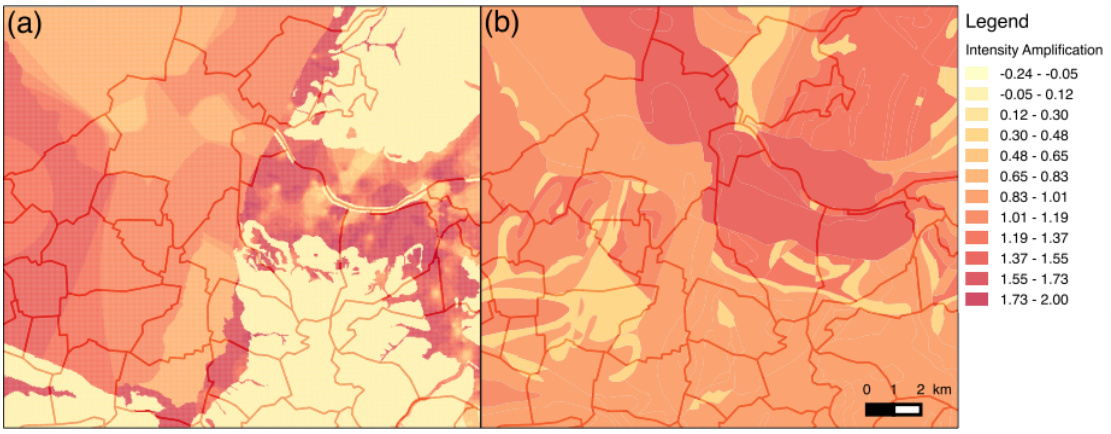

Fig. 13 Amplification map in Basel in terms of macroseismic intensity increments. a) this study; b) nation-wide amplification map (Fäh et al., 2011).

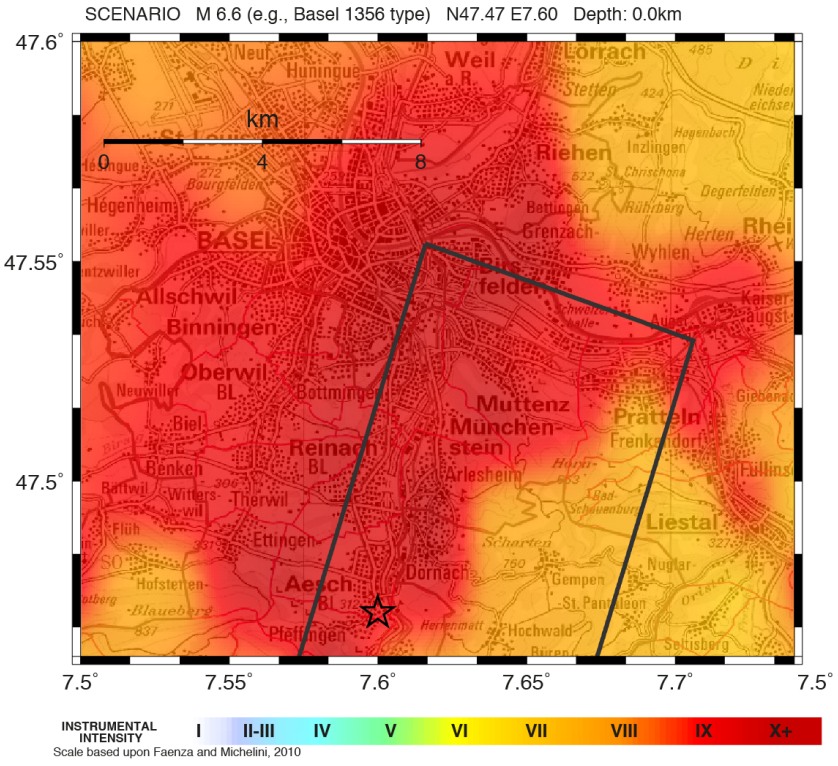

Fig. 14 ShakeMap of the possible repetition of the 1356 M_W 6.6 event, computed as explained in the text. The star is the ECOS-09 epicentre, while the solid grey lines show the surface projection of the ruptured fault in the city area.

7. Discussion and conclusions

The recent recordings of high-quality permanent and temporary accelerometer stations have significantly improved our understanding and representation of earthquake ground-motion amplification in the municipal area of Basel. We estimated the amplification at each station using empirical spectral modelling of records from the whole permanent network. This method is complementary to site characterization and overcomes limitations of SSRs, particularly the absence of rock reference station. It accounts for 2D/3D effects naturally included in the used earthquake records but the resolution is too low to map these rapidly changing effects at the edge of the basin and close to faults (Panzera et al., 2016). Moreover, it is only based on the recording of weak motions and cannot account for non-linear behaviour of the sediments as detailed numerical site response analysis could.

We identified the most important features that play a role in the site amplification. In the Rhine Graben, the interface with the Mesozoic bedrock and 2D/3D effects; outside the Rhine Graben, the depth of the Quaternary sediments and their material properties. This should be used to improve the 3D numerical models in the future. However, questions are remaining regarding the interpretation of the bedrock since our assessment is based on a single borehole. For instance, the interface between the upper and the lower Tertiary, also showing a strong velocity contrast, could also produce a resonance frequency at other locations in the basin. More research using the large available H/V dataset and 3D modelling should be performed to achieve a complete understanding of site effects in this area. This shows again the complementarity of ESM technique and geophysical site characterization.

We could verify the amplification functions derived in 2006 microzonation and propose improvements. We placed emphasis on the importance of using monitoring stations to verify microzonation studies. We proposed a new method to derive amplification maps from the individual amplification functions. In the Rhine Graben, where amplification varies only little in space, we interpolated the amplification functions obtained at each station of the network; outside the Rhine Graben, we used an amplification functional form obtained from the individual functions at the accelerometric sites coupled with fundamental frequencies mapped through single station measurements and H/V analysis. Compared to the 2006 microzonation, a larger spatial variability of the amplification and more extreme values have been identified. Although derived under low-strain seismic excitation, the amplification maps resulting from this study can be tentatively used as input to shaking scenarios for loss assessment, eventually produced in real-time. The high-resolution (40 m) of the amplification maps presented in this manuscript is optimally tailored at earthquake risk assessment at the building level.

Acknowledgements

This work has been funded by the Crisis Organization of the Canton Basel-Stadt. The authors thank Geo-Energie Suisse AG who provided the sonic logging data and the GeORG project team who provided geological data (http://www.geopotenziale.eu/). The authors are grateful to the two anonymous reviewers who helped improve the paper.

References

Bora, S. S., Scherbaum, F., Kuehn, N., Stafford, P. (2016). On the Relationship between Fourier and Response Spectra: Implications for the Adjustment of Empirical Ground-Motion Prediction Equations (GMPEs), *Bulletin of the Seismological Society of America*, **106**(3), 1235-1253.

Bora, S. S., Scherbaum, F., Kuehn, N., Stafford, P., Edwards, B. (2015). Development of a Response Spectral Ground-Motion Prediction Equation (Gmpe) for Seismic-Hazard Analysis from Empirical Fourier Spectral and Duration Models, *Bulletin of the Seismological Society of America* **105**, 2192-2218.

Boore, D. M. (2003). Simulation of Ground Motion Using the Stochastic Method, *Pure and Applied Geophysics* **160**, 635-676.

Borcherdt, R.D. (1970). Effects of local geology on ground motion near San Francisco Bay. Bull. Seismol. Soc. Am. 60, 29–61.

Burjánek, J., Edwards, B. Fäh, D. (2014). Empirical evidence of local seismic effects at sites with pronounced topography: a systematic approach. *Geophys. J. Int.* **197,** 608–619.

Cadet, H., Bard, P., Duval, A.-M., Bertrand, E. (2012). Site effect assessment using KiK-net data: Part 2-site amplification prediction equation based on f0 and Vsz. *Bulletin of Earthquake Engineering*, *10*(2), 451–489. doi:10.1007/s10518-011-9298-7

Campbell, K. W. (2003). Prediction of Strong Ground Motion Using the Hybrid Empirical Method and Its Use in the Development of Ground-Motion (Attenuation) Relations in Eastern North America, *Bulletin of the Seismological Society of America* **93**, 1012-1033.

Cartwright, D. E., Longuet-Higgins, M. S. (1956). The statistical distribution of the maxima of a random function, Proc R Soc Lon Ser-A 237, 212-232.

Cauzzi, C., Edwards, B., Fäh, D., Clinton, J., Wiemer, S., Kastli, P., Cua, G., Giardini, D. (2015). New predictive equations and site amplification estimates for the next-generation Swiss ShakeMaps. *Geophysical Journal International*, *200*, 421–438. doi:10.1093/gji/ggu404

Cauzzi, C., Clinton, J., (2013). A High- and Low-Noise Model for High-Quality Strong-Motion Accelerometer Stations. Earthq. Spectra 29, 85–102. doi:10.1193/1.4000107

Clinton, J., Cauzzi, C., Fäh, D., Michel, C., Zweifel, P., Olivieri, M., Cua, G., Haslinger, F., Giardini, D. (2011). The Current State of Strong Motion Monitoring in Switzerland, in: Akkar, S., Gülkan, P., van Eck, T. (Eds.), Earthquake Data in Engineering Seismology, Geotechnical, Geological, and Earthquake Engineering. Springer Netherlands, Dordrecht, pp. 219–233. doi:10.1007/978-94-007-0152-6

Cressie, N. (1993). Statistics for spatial data: John Wiley Sons, New York, 900 p.

Deichmann, N., Giardini, D. (2009). Earthquakes Induced by the Stimulation of an Enhanced Geothermal System below Basel (Switzerland). Seismol. Res. Lett. 80, 784–798. doi:10.1785/gssrl.80.5.784

Diehl, T., Deichmann, N., Clinton, J., Kästli, P., Cauzzi, C., Kraft, T., Behr, Y., Edwards, B., Guilhem, A., Korger, E., Hobiger, M., Haslinger, F., Fäh, D., Wiemer, S. (2015). Earthquakes in Switzerland and surrounding regions during 2014. Swiss J. Geosci. 108, 425–443. doi:10.1007/s00015-015-0204-1

Edwards, B., Cauzzi, C., Danciu, L., Fäh, D. (2016). Region-specific Assessment, Adjustment and Weighting of Ground Motion Prediction Models: application to the 2015 Swiss Seismic Hazard Maps. *Bulletin of the Seismological Society of America, 106*(4), 1840-1857. doi:10.1785/0120150367

Edwards, B., Kraft, T., Cauzzi, C., Kästli, P., Wiemer, S. (2015a). Seismic Monitoring and Analysis of Deep Geothermal Projects in St Gallen and Basel, Switzerland, *Geophysical Journal International* **201**, 1020-1037, doi: 10.1093/gji/ggv059.

Edwards, B., Ktenidou, O.-J., Cotton, F., Abrahamson, N., Van Houtte, C., Fäh, D. (2015b). Epistemic uncertainty and limitations of the κ_0 model for near-surface attenuation at hard rock sites. *Geophysical Journal International*, *202*(3), 1627–1645. doi:10.1093/gji/ggv222

Edwards, B., Michel, C., Poggi, V., Fäh, D. (2013). Determination of Site Amplification from Regional Seismicity: Application to the Swiss National Seismic Networks. *Seismological Research Letters*, *84*(4), 611–621. doi:10.1785/0220120176

Edwards, B., Fäh, D. (2013). A Stochastic Ground-Motion Model for Switzerland. *Bulletin of the Seismological Society of America*, *103*(1), 78–98. doi:10.1785/0120110331

Faenza, L., Michelini, A. (2011). Regression analysis of MCS intensity and ground motion spectral accelerations (SAs) in Italy. *Geophysical Journal International*, *186*, 1415–1430. doi:10.1111/j.1365-246X.2011.05125.x

Faenza, L., Michelini, A. (2010). Regression analysis of MCS intensity and ground motion parameters in Italy and its application in ShakeMap. *Geophysical Journal International*, *180*, 1138–1152. doi:10.1111/j.1365-246X.2009.04467.x

Fäh, D., Giardini, D., Kästli, P., Deichmann, N., Gisler, M., Schwarz-Zanetti, G., Alvarez-Rubio, S., Sellami, S., Edwards, B., Allmann, B., Bethmann, F., Wössner, J., Gassner-Stamm, G., Fritsche, S., Eberhard, D. (2011). ECOS-09 Earthquake Catalogue of Switzerland Release 2011. Report and Database. Public catalogue, 17.4.2011. Swiss Seismological Service ETH Zürich, Report SED/RISK/R/001/20110417.

Fäh, D., Gisler, M., Jaggi, B., Kästli, P., Lutz, T., Masciadri, V., Matt, C., Mayer-Rosa, D., Rippmann, D., Schwarz-Zanetti, G., Tauber, J., Wenk, T. (2009). The 1356 Basel earthquake: an interdisciplinary revision. *Geophysical Journal International*, *178*(1), 351–374. doi:10.1111/j.1365-246X.2009.04130.x

Fäh, D., Wenk, T. (2009). Mikrozonierung für die Kantone Basel Stadt und Basel Landschaft : Optimierung der Form der Antwortspektren und der Anzahl der Mikrozonen : Abschlussbericht: Teilbericht B, WTH Zurich.

Fäh, D., Steiner, B., Havenith, H.-B., Steimen, S., Huggenberger, P., Fäh, E. (2006). *INTERREG III Projekt: Erdbebenmikrozonierung am südlichen Oberrhein. Teilbericht 1: Zoneneinteilung*. doi:10.3929/ethz-a-006411876

Fäh, D., Havenith, H. (2006). *INTERREG III Projekt: Erdbebenmikrozonierung am südlichen Oberrhein. Teilbericht 5: Bestimmung der zonenspezifischen Antwortspektren*. doi:10.3929/ethz-a-006412190

Fäh, D., Huggenberger, P. (2006). *INTERREG III Projekt: Erdbebenmikrozonierung am südlichen Oberrhein: Zusammenfassung.* doi: 10.3929/ethz-a-006412199

Fäh, D., Kind, F., Lang, K., Giardini, D. (2001). Earthquake scenarios for the city of Basel. *Soil Dynamics and Earthquake Engineering*, *21*, 405–413.

Fäh, D., Rüttener, E., Noack, T., Kruspan, P. (1997). Microzonation of the city of Basel. *Journal of Seismology*, *1*, 87–102.

Ferry, M., Meghraoui, M., Delouis, B. Giardini, D. (2005). Evidence for Holocene palaeoseismicity along the Basel-Reinach active normal fault (Switzerland): A Seismic source for the 1356 earthquake in the Upper Rhine graben. *Geophys. J. Int.* **160,** 554–572.

GeORG project team (2013) *Geopotenziale des tieferen Untergrundes im Oberrheingraben, Fachlich-Technischer Abschlussbericht des INTERREG-Projekts GeORG, Teile 1–4. – Internet (PDF documents: http://www.geopotenziale.eu).*

Giardini, D. (2009). Geothermal quake risks must be faced. Nature 462, 848–849.

Gisler, M., Fäh, D. (2011). *Grundlagen des Makroseismischen Erdbebenkatalogs der Schweiz Band 2: 1681-1878* (Schweizerischer Erdbebendienst). doi:10.3218/3407-3

Grünthal, G., Musson, R. M. W., Schwartz, J., Stucchi, M. (1998). *European Macroseismic Scale 1998* (Vol. 15). Luxembourg: Cahiers du Centre Européen de Géodynamique et de Séismologie.

Häring (2006), Geothermie-Sondierbohrung Otterbach 2, Basel, Technical report, Geothermal Explorers Ltd.

Havenith, H.-B., Fäh, D., Polom, U., Roullé, A. (2007). S -wave velocity measurements applied to the seismic microzonation of Basel, Upper Rhine Graben. *Geophysical Journal International*, *170*(1), 346–358. doi:10.1111/j.1365-246X.2007.03422.x

Kind, F., Fäh, D., Giardini, D. (2005). Array measurements of S-wave velocities from ambient vibrations. *Geophysical Journal International*, *160*(1), 114–126. doi:10.1111/j.1365-246X.2005.02331.x

Kind, F. (2002). *Development of Microzonation Methods: Application to Basle, Switzerland*. PhD Thesis Nr. 14548, Swiss Federal Institute of Technology Zürich.

Liu, L., Pezeshk, S. (1999). An improvement on the estimation of pseudoresponse spectral velocity using RVT method, B Seismol Soc Am 89, 1384-1389.

Michel, C., Fäh, D. (2016). Basel earthquake risk mitigation – Computation of scenarios for school buildings, Technical Report, ETHZ-SED, Zürich, Switzerland, 69 pp. doi: 10.3929/ethz-a-010646514

Michel, C., Edwards, B., Poggi, V., Burjánek, J., Roten, D., Cauzzi, C., Fäh, D. (2014). Assessment of Site Effects in Alpine Regions through Systematic Site Characterization of Seismic Stations. *Bulletin of the Seismological Society of America*, *104*(6), 2809–2826. doi:10.1785/0120140097

Opršal, I., Fäh, D., Mai, P. M., Giardini, D. (2005). Deterministic earthquake scenario for the Basel area: Simulating strong motions and site effects for Basel, Switzerland. *Journal of Geophysical Research*, *110*(B4), 1–19. doi:10.1029/2004JB003188

Panzera F, Lombardo G, Monaco C (2016). New evidence of wavefield polarization on fault zone in the lower NE slope of Mt. Etna. Italian Journal of Geoscience, *135*(2), 250-260, doi:10.3301/IJG.2015.22

Poggi, V., Edwards, B., Fäh, D. (2011). Derivation of a Reference Shear-Wave Velocity Model from Empirical Site Amplification. *Bulletin of the Seismological Society of America*, *101*(1), 258–274. doi:10.1785/0120100060

Ripperger, J., Kästli, P., Fäh, D., Giardini, D. (2009). Ground motion and macroseismic intensities of a seismic event related to geothermal reservoir stimulation below the city of Basel - observations and modelling. *Geophysical Journal International*, *179*(3), 1757–1771. doi:10.1111/j.1365-246X.2009.04374.x

Schwarz-Zanetti, G., Fäh, D. (2011). *Grundlagen des Makroseismischen Erdbebenkatalogs der Schweiz Band 1: 1000-1680* (Schweizerischer Erdbebendienst). doi:10.3218/3407-3

Steimen, S., Fäh, D., Kind, F., Schmid, C., Giardini, D. (2003). Identifying 2D Resonance in Microtremor Wave Fields. *Bulletin of the Seismological Society of America*, *93*(2), 583–599.

Swiss Seismological Service (SED) at ETH Zurich (2015a). *Swiss National Probabilistic Seismic Hazard Assessment 2015*. Zurich: Federal Institute of Technology (retrieved on 23/05/2016 from http://www.seismo.ethz.ch/prod/Erdbebengefaehrdungsmodell_2015/index_EN)

Swiss Seismological Service (SED) at ETH Zurich (2015b). The Site Characterization Database for Seismic Stations in Switzerland. Zurich: Federal Institute of Technology. doi: 10.12686/sed-stationcharacterizationdb (retrieved on 04/02/2016 from http://stations.seismo.ethz.ch)

Ullah, S., Bindi, D., Pittore, M., Pilz, M., Orunbaev, S., Moldobekov, B., Parolai, S. (2013). Improving the spatial resolution of ground motion variability using earthquake and seismic noise data: The example of Bishkek (Kyrgyzstan). Bull. Earthq. Eng. 11, 385–399. doi:10.1007/s10518-012-9401-8

Wald, D.J., Quitoriano, V., Heaton, T.H., Kanamori, H., Scrivner, C.W. Worden, C.B. (1999). TriNet "ShakeMaps": rapid generation of peak ground motion and intensity maps for earthquakes in Southern California, Earthq. Spectra, 15(3), 537–555.

Worden, C.B., Wald, D.J., Allen, T.I., Lin, K., Garcia, D. Cua, G. (2010). A revised ground-motion and intensity interpolation scheme for ShakeMap. Bull. seism. Soc. Am., 100(6), 3083–3096.